Implementation of Finite Strain-Based Constitutive Formulation in LLLNL-DYNA3D to Predict Shockwave Propagation in Commercial Aluminum Alloys AA7010

M K Mohd Nor[*1], N Ma'at[1], K A Kamarudin[1], A E Ismail[1]

Crashworthiness and Collision Research Group, Engineering Mechanics Department, Faculty of Mechanical and Manufacturing Engineering, Universiti Tun Hussein Onn Malaysia, 86400 Parit Raja, Batu Pahat, Johor, Malaysia

E-mail: khir@uthm.edu.my

Abstract. The constitutive models adopted to represent dynamic plastic behaviour are of great importance in the current design and analysis of forming processes. Many have studied this topic, leading to results in various technologies involving analytical, experimental and computational methods. Despite of this current status, it is generally agreed that there is still a need for improved constitutive models. There are still many issues relating to algorithm implementation of the proposed constitutive model in the selected code to represent the proposed formulation. Using this motivation, the implementation of a new constitutive model into the LLNL-DYNA3D code to predict the deformation behaviour of commercial aluminium alloys is discussed concisely in this paper. The paper initially explains the background and the basic structure of the LLNL-DYNA3D code. This is followed by a discussion on the constitutive models that have been chosen as the starting point for this work. The initial stage of this implementation work is then discussed in order to allow all the required material data and the deformation gradient tensor **F** to be read and initialised for the main analysis. Later, the key section of this implementation is discussed, which mainly relates to subroutine f3dm93 including equation of state (EOS) implementation. The implementation of the elastic-plastic part with isotropic plastic hardening, which establishes the relationship between stress and strain with respect to the isoclinic configuration $\overline{\mathbf{\Omega}}_i$ in the new deviatoric plane, is then presented before the implemented algorithm is validated against Plate Impact test data of the Aluminium Alloy 7010. A good agreement is obtained in each test.

1. Introduction

In practice, in the real world, most of the engineering materials such as composites and sheet metal components, manufactured using sheet metal forming processes, are orthotropic. Sheet forms of aluminum alloy are examples of orthotropic materials. Furthermore, many engineering materials such as fibre-reinforced elastomers or glassy polymers exhibit orthotropic behaviour while undergoing large elasto-plastic deformation which can be observed at the unit-cell level due to the preferred orientations as a result of various manufacturing processes. At quasi-static rates of strain, this behaviour has been studied by few researches as published in [1] and [2] while significant contribution to investigate the behaviour of materials that impacted with dynamic shock loading can be observed in [3-9]. The awareness that anisotropic materials has broad engineering applications have brought to others constructive research on the behaviour of such materials exerted with high impact velocity that

creates shockwave propagation in the materials, see for example [9-13]. A brief review of researches focusing on shock response of anisotropic materials can be found in [14]. The constitutive models intended to represent dynamic plastic behaviour are of great importance in the current design and analysis of forming processes due to various engineering application, [15].

Much research has been carried out in respect to complex structures under dynamic loading conditions, leading to results in various technologies involving analytical, experimental and computational methods in various applications of automotive, aerospace and manufacturing processes. The implementation of constitutive formulation in the selected finite element code is one of the real challenges to meet the requirements in current applications, however rarely discussed in details. It is important to ensure findings in this field can really enhance the prediction capability of simulation tools. Using this motivation, this paper discusses the implementation works of a newly constitutive formulation into the LLNL-DYNA3D code. The approach is helpful to guide the implementation of the other constitutive model in this code. Further, the proposed framework can be beneficial to track the implementation method in the other finite element code.

The important features of the chosen constitutive model for implementation are the multiplicative decomposition of the deformation gradient and a new Mandel stress tensor combined with the new stress tensor decomposition. The elastic free energy function and the yield function are defined within an invariant theory by means of the introduction of the evolving structural tensors used to describe the material symmetry. The plastic orthotropy is characterised by the Hill's yield criterion. The thermally micromechanical-based model, Mechanical Threshold Model (MTS) is adopted as a referential curve to control the yield surface expansion that accounts for isotropic plastic hardening. This constitutive model is developed and integrated in the isoclinic intermediate configuration. The development of this constitutive model is first published in [16] and further developed in [17] and [18].

2. Background of LLNL-DYNA3D

This section presents the background of the LLNL-DYNA3D code, followed by an overview of the main structure in the following section. DYNA3D is basically an explicit finite element code that is used to study transient dynamic response. It is also known as a hydrocode, or an explicit three-dimensional finite element simulation code to solve finite deformation problems and inelastic materials that occur in a short time scale. This hydrocode is formulated based on the conservation of energy, mass and momentum equations. This code was initially developed at Lawrence Livermore National Laboratory (LLNL), and it has been widely used in LLNL and in many industries. In addition, the public DYNA3D code is maintained and developed by the Methods Development Group at LLNL.

DYNA3D is capable of formulating a variety of elements such as one dimensional truss, one dimensional beam elements, three-dimensional continuum elements and many more. Moreover, DYNA3D offers plenty of constitutive models and equations of state, hence is able to represent a wide range of material behaviour, and also has the capability to model finite element analysis with a variety of modelling options. Equally, DYNA3D allows different bodies to interact as it contains several contact-impact algorithms.

2.1. Structure of LLNL-DYNA3D

The implementation of the new constitutive model is quite difficult to perform. Anyone who needs to modify the code must first learn the structure of the LLNL-DYNA3D code. Particularly, it is very useful to understand of the COMMON block, as well as the way that FORTRAN stores data in arrays when learning the DYNA3D code.

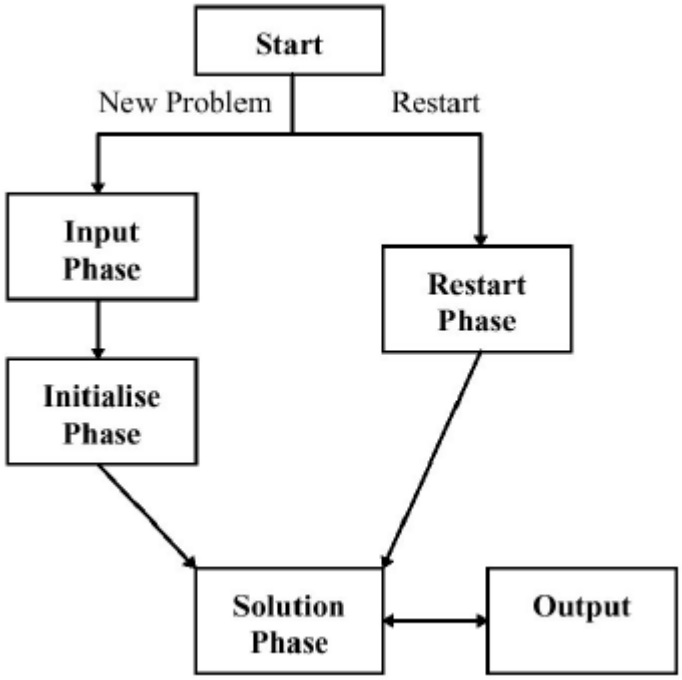

Figure 1. Basic Structure of DYNA3D code

The basic structure of the 1995 release of the public DYNA3D program is shown in Figure 1. It can be seen that the structure of the DYNA3D code can be divided into five main sections: Input, Initialise, Restart, Solution and Output. A good overview of the DYNA3D code also can be found in [19] and [20]. The other available documentation for DYNA3D is the User Manual [21] and the Theoretical Manual [22].

2.2. Data Handling

At the core of DYNA is the central database which consists of single large array that is dimensioned at the start of the program, called a. The size of this array places an upper limit on the size of the problem that the problem can handle.

All the solution variables are stored in the DYNA database that consists of data such as the stress tensor, contact surface segments, nodal coordinates, velocities, positions and element connectivity. The data stored is required or updated during each time step. DYNA calculates a number of pointers to access the data in the database. Each pointer denotes an integer variable that contains the location of each variable or array stored in the database. For instance, lc9 is the pointer to the nodal velocities array. Suppose v(1,1), the *x* velocity of node 1, is entry 500 in a means that 500 is the value of lc9.

The pointers are calculated during the input phase of DYNA program. Once the numbers of nodes and elements in the model are known, and what options are active have been determined, DYNA will calculates the value of the pointers. The value of pointer lc10, which follows immediately pointer lc9, refers to the value of lc9 plus the number of degrees of freedom that each node has times the total number of nodes.

DYNA variables are packed and unpacked from the database via CALL statements. This option is rarely used to pass variables between subroutines, unless variables are being packed and unpacked from the main database. The other way that variables are passed between subroutines is by using COMMON blocks. A comprehensive description regarding the of the DYNA3D data handling also can be found in [20].

3. Overview of the Reference Constitutive model

To implement the proposed constitutive model, two constitutive models that are available in LLNL-DYNA3D code have been taken as references. The first is the General Anisotropic Elastic-Plastic; Material Type 33. This constitutive model is used as a starting point of this implementation. The other one is a recent constitutive model developed in the code; Material Type 97.

Material Type 33 was originally developed at LLNL. It combines the orthotropic elastic model, Material Type 2 with Hill's yield criterion. The algorithm of this constitutive model consists of a new elastic-plastic stiffness matrix or a constitutive matrix calculation at each time step. In addition, a tangent stiffness algorithm and an associated plasticity are employed in this constitutive model. Furthermore, an elliptic shape of the yield surface is assumed, due to the orthotropic Hill's parameters.

Regarding Material Type 97, this consists of the initial implementation of the new stress tensor decomposition into LLNL-DYNA3D [23]. This constitutive model was developed based on the Fiber Composite with Damage constitutive model; Material Type 22. However, the implementation of Material Type 97 excluded the damage model of the Material Type 22. In order to more reasonably capture the plastic deformation behaviour and the shock wave propagation of materials under high velocity impact, this constitutive model was combined with an equation of state (EOS).

3.1. Material Type 33

The description of Material Type 33 is discussed in this section. Collectively, there are six main subroutines that deal with this constitutive model; solde, matin, iniltz, inse33, sets33 and f3dm33.

The subroutine matin is used to read in the data from the input file. This subroutine consists of a call command to call the subroutine sets33. This subroutine is responsible for reading all the specific material data that are assigned for Material Type 33.

In the subroutine iniltz, all subroutines that are required to initialise for the solution phase initialisation are called. The subroutine that initialises the values related to Material Type 33 is inse33. This subroutine calculates the transformation matrix – the q matrix. This matrix transforms axes from element to material axes.

During the solution phase, the subroutine fem3d is called from the subroutine soltn. As has been mentioned, a different subroutine is called from the subroutine fem3d depending on the basic type of element. Referring to Material Type 33, a subroutine solide is called from fem3d. Subsequently, subroutine solde is called from the subroutine solide to process solid elements for the Material Type 33 analysis.

In addition, several subroutines are specifically called for each constitutive model, depending on their formulation in the subroutine solde. It is from this point in this subroutine that the program splits to consider different constitutive models. For Material Type 33, five subroutines are called, which are hvpac1, rstrss, f3dm33, bulkq, engbrk and hvpac2. Most of the DYNA3D subroutines in fact are developed for a special function – hence, they are used when a specific option is activated.

The subroutine rstrss calculates the rotated stress tensor. The subroutine f3dmxx is the main subroutine for each constitutive model in DYNA3D, where xx refers to the material type number. This subroutine calculates the new stress tensor and the element's internal energy. Detailed explanations of subroutine f3dm33 can be found in [20]. A concise overview of the other constitutive models available in LLNL-DYNA3D code is given in the Theoretical Manual [22]. Subroutine bulkq calculates the critical timestep and bulk viscosity. Meanwhile, the subroutine engbrk is used to calculate the kinetic energy for each element.

3.2. Material Type 97

The description of the Material Type 97 subroutine is discussed in this section. The explanation is focused on solid elements, hence little difference can be observed with respect to the previous discussion in terms of material data handling. Material Type 97 combines the formulation of the new stress tensor decomposition with an EOS – hence, it must be connected to additional subroutines in LLNL-DYNA3D.

First, it should be noted that any constitutive model that uses an EOS formulation calculates the pressure component in a separate set of subroutines. Subroutine f3dmxx of such a constitutive model only calculates the deviatoric part of the constitutive relation. On the other hand, it can be observed that any constitutive model which does not link with an EOS formulation calculates the volumetric (pressure) part of the stress tensor in the subroutine f3dmxx.

With respect to Material Type 97, it is linked with subroutines solde, matin, iniltz, inse97, sets97, f3dm97, bulkq, and engbrk. Additionally, subroutines sueos, hieupd97 and eqos97 are called from the subroutine solde for an EOS implementation of this constitutive model.

Since Material Type 22 is adopted as a starting point for this constitutive model implementation, the subroutines inse97 and sets97 are copied from subroutines inse22 and sets22, respectively. Subroutine bulkq is used to calculate the new critical time step and bulk viscosity, while the subroutine engbrk calculates the momentum and kinetic energy. The subroutine sueos calculates the speed of sound of the element. In addition, the subroutines hieupd97 and eqos97 calculate the trial value of the internal energy, and the new pressure and internal energy, respectively.

The implementation of Material Type 97 follows the formulation of the new stress tensor decomposition, where the new generalised pressure for orthotropic materials is introduced. However, the new expression of orthotropic pressure defined in Mohd Nor et al. (2013) [16] cannot directly be calculated in the subroutine f3dm97, since only the deviatoric stress tensor is calculated and updated in this subroutine.

This implementation requires modifications to subroutines hieupd97 and eqos97 in order to calculate the proposed orthotropic pressure. The description of this implementation is rigorously discussed in the following section, where the implementation of the constitutive model is presented.

4. Preliminary Implementation of Material Type 93

The implementation of the constitutive model proposed in [16] and [17] involved the modification of several subroutines in the LLNL-DYNA3D code. The implementation of this constitutive model in fact not only included subroutines that directly related to Material Types 33 and 97, but contained modifications on some other subroutines in LLNL-DYNA3D. The constitutive model is named Material Type 93. This identification 93 is used for subroutines that are created specifically for this constitutive model.

4.1. Input Parameters

The Hill's yield criterion and the MTS model of the proposed formulation are combined to characterise the proposed 'micro-macro' constitutive model. This combination requires more input parameters compared to existing Material Types 33 and 97.

As noted previously, Material Type 33 is adopted as the starting point for the new constitutive model implementation. Therefore, all subroutines specifically related to this constitutive model were renamed and duplicated to reflect Material Type 93. The subroutines that were duplicated are f3dm33, sets33 and inse33, so were changed to f3dm93, sets93 and inse93, respectively. For the sake of brevity, the input parameters of this constitutive model that are arranged in the material cards and read into the subroutine matin, are maintained in the same way.

On the other hand, the MTS model requires 31 input parameters (material properties). To support the MTS material properties, five extra material cards are added for Material Type 93. In LLNL-DYNA3D, material data or input parameters of any constitutive model are stored in cm array. Since Material Type 33 already used the maximum six material cards stored in cm array, an additional cm array is required for the extra material cards of the new constitutive model.

To read in the extra material cards for the MTS material properties of the new constitutive model, cm2 array is initialised in the subroutine dynai by using pointer n3a. This pointer is used to mark the beginning of where auxiliary material data are stored in the main database. This pointer is initialised in dynai as follows:

$$n3a=n3+48*nmmat \quad (1)$$

This means the extra material cards data are stored between n3 and n4a. Equally, there are 48 spaces available to support all of the additional material properties. In addition, a(n3a) is included in a call statement to the subroutine matin in this subroutine (dynai). Accordingly, cm2 is added in the matin's argument.

By using the cm2 array, the MTS material properties of the new constitutive model can be conveniently introduced without disturbing the existing material cards that are copied from Material Type 33. A new section is added in subroutine matin to read in all the material data that are assigned for Material Type 93, where 11 material cards are introduced all together.

Subsequently, a call to the subroutine sets93 is further added in the subroutine matin in order to read in all the specific material data of the Material Type 93. Equally, a specific line is added in the subroutine sets93 to read the extra material cards stored in the cm2 array.

4.2. Deformation Gradient

The implementation of the deformation gradient is really important, as the formulation of the new constitutive model is defined within this framework. Generally speaking, the implementation of this tensor follows the explanation in the LLNL-DYNA3D source code file; prepare_bricks.F90.

The prepare_bricks.F90 contains several subroutines which are called from the other subroutines in the LLNL-DYNA3D code when certain specific formulations are required. For instance, in this case, two main subroutines contained in the prepare_bricks.F90: init_brick_edata and cal_brick_defgrad are called to ensure the deformation gradient tensor is available for the new constitutive model analysis.

The implementation of the deformation gradient starts with the modification in the subroutine matin, where all the material data for any constitutive model is read in. In this subroutine in fact, DYNA3D must be systematically instructed that the deformation gradient tensor is required in the Material Type 93 analysis.

For this purpose, the subroutine initial_brick_edata in the file prepare_bricks.F90 is called by the subroutine matin. It is used to set up space to hold element data such as hourglass control variables, the variables required for the deformation gradient calculation, etc. In the following, the new constitutive model identification 93 is put in the 'deform' option of matin to set data for the deformation gradient calculation.

In addition, the subroutine initial_brick_edata also wants to know how anisotropic the constitutive model is. Therefore, the second option of 'ortho' in the subroutine matin is assigned to Material Type 93. This means that if orthotropic properties are assigned, then the stiffness can differ from element to element of this constitutive model. For instance, if the properties are temperature dependent, the value of temperature can differ between elements.

The deformation gradient tensor is initialised in the subroutine inse93. In this subroutine, a call to the subroutine init_brick_edata is made to load element data for the calculation of the deformation gradient. Consequently, extra variables are added in the inse93's arguments to support the deformation gradient initialisation: mat, elem, ipt. These variables refer to the current material number, the current internal element number and the current integration point, respectively.

To ensure the deformation gradient tensor is available to process solid elements, the subroutine solde has to be modified. In this subroutine, a call to the subroutine cal_brick_defgrad is made. This is the main subroutine that calculates the deformation gradient tensor for brick elements.

Since the deformation gradient tensor is required in the subroutine f3dm93 of the new constitutive model, a call to cal_brick_defgrad is made just before a call to f3dm93 and immediately after a call to the subroutine hvpac1. This means no call statement is added to call the subroutine rstrss, and this is discussed later.

Finally, the deformation gradient tensor is passed to the subroutine f3dm93 via a common block def_grad. This common block consists of nine components of the deformation gradient tensor **F**:

$$F_{ij} = \begin{bmatrix} F_{11} & F_{12} & F_{13} \\ F_{21} & F_{22} & F_{23} \\ F_{31} & F_{32} & F_{33} \end{bmatrix} \quad (2)$$

5. Equation of State (EOS)

The implementation of equation of state (EOS) that is combined with the proposed constitutive model is discussed in this section. EOS provides a special treatment upon the volumetric (pressure) part of the stress tensor. Since this constitutive model uses a new generalised pressure for orthotropic materials, a few modifications are required on this implementation.

Since the subroutine f3dm93 calculates only the deviatoric part of the constitutive relation, the pressure part of the stress tensor has to be calculated separately in the other subroutines. Therefore, some changes had to be made to decouple the volumetric and deviatoric parts of the stress tensor.

5.1. General Implementation of EOS

The first step of EOS implementation is to ensure the EOS option is specified for Material Type 93 in the subroutine matin. Recalling the initial implementation of Material Type 97, the EOS implementation for the proposed constitutive model is restricted to work only with EOS type 1 (Linear Polynomial) and 4 (Gruneisen).

Subsequently, the EOS parameters need to be initialised in the subroutine inse93. These data are stored as auxiliary variables in the subroutine blkdat. These variables are then passed to the subroutine f3dm93 via common/aux14/. These values are arranged after six components of the Cauchy stress tensor and the equivalent plastic strain. By passing the EOS parameters using the common/aux14/, these values can be used in other subroutines related to Material Type 93.

Apart from subroutines bulkq and engbrk, additional subroutines have to be called from the subroutine solde for EOS implementation: subroutines sueos, hieupd93 and eqos93.

The subroutine f3dm93 was structured and modified to provide all the data required for EOS formulation. For instance, to pass the value of old stress tensors to the subroutine hieupd93, these tensors are calculated and then stored in the second to seventh entry of the common/aux11/.

In addition, the algorithm has to be critically developed to ensure that subroutine f3dm93 always updates the deviatoric part of the stress tensor. However, no modifications are required to update the stress tensor when a material starts to yield (plasticity part), since the plastic deformation causes only a change in shape (incompressibility).

At the end of EOS implementation, the updated orthotropic pressure of the full stress tensor is known. The subroutine hvpac2 then is called from subroutine solde to store the new stress tensor and the auxiliary variables of the proposed constitutive model in the DYNA3D main database.

5.2. Orthotropic Pressure Implementation

A series of modifications were required to reflect the formulation of the new orthotropic pressure, since the LLNL-DYNA3D code considers only the conventional volumetric part of the stress tensor. The implementation of the new orthotropic pressure requires modifications on subroutines f3dm93, hieupd93 and eqos93. In addition, it is important to remember the formulation of EOS is performed in the current configuration $\boldsymbol{\Omega}_t$.

Assuming that all of the required data have been successfully passed and calculated in subroutine f3dm93, the first step is to calculate the old stresses. These values are required in subroutine hieupd93. To ensure that subroutine f3dm93 only calculates and updates a deviatoric stress tensor, the deviatoric part of the new stress tensor decomposition is used:

$$S_{ij} = \sigma_{ij} + \tilde{P}\psi_{ij} \tag{3}$$

The ψ_{ij} tensor is fully defined by the material elastic stiffness properties c_{ij} using the following equation

$$\psi_{(ii)} = \frac{c_{i1} + c_{i2} + c_{i3}}{\sqrt{\frac{(c_{11} + c_{12} + c_{13})^2 + (c_{12} + c_{22} + c_{23})^2 + (c_{13} + c_{23} + c_{33})^2}{3}}} \tag{4}$$

Repeated indices in brackets in the above equation indicate no summation. The value of this tensor is stored in the common/aux14/ to be easily passed between the Material Type 93 subroutines. The volumetric part of equation (3) is replaced by the pressure that was calculated from EOS formulation $\tilde{P}_{EOS}$ to reflect the proposed formulation for this constitutive model. Therefore, equation (3) can be rewritten as follows:

$$S_{ij} = \sigma_{ij} + \tilde{P}_{EOS}\psi_{ij} \tag{5}$$

This equation is used to calculate the old stresses of the proposed constitutive model and stored in the common/aux11/ to be used later in the subroutine hieupd93. The old pressure po meanwhile is stored as the first entry of this common block. The ultimate purpose of the subroutine hieupd93 is to calculate the trial value of the internal energy e^*, such that

$$e^* = e^n - \frac{1}{2}P^n \boldsymbol{V}^{n+1/2}\mathbf{D}_\psi{}^{n+1/2}\Delta t^{n+1/2} + \boldsymbol{V}^{n+1/2}\mathbf{S}^{n+1/2}\mathbf{D}'^{n+1/2}\Delta t^{n+1/2} \tag{6}$$

where P, $\boldsymbol{V}$, $\mathbf{S}$ and $\mathbf{D}$ refer to pressure, velocity, deviatoric stress and rate of deformation tensor respectively. $\mathbf{D}_\psi$ is calculated by referring to the definition of the new orthotropic pressure as follows:

$$\mathbf{D}_\psi = \psi_{11}D_{11} + \psi_{22}D_{22} + \psi_{33}D_{33} \tag{7}$$

The trial value of the internal energy is named epx2 and stored in the common/aux14/. This value is then used in the subroutine eqos93 to calculate the final internal energy epx2 and finally updates the orthotropic pressure $\tilde{P}_{EOS}$. At the end of the subroutine eqos93, the updated orthotropic pressure is further used to update the full stress tensor. This full stress tensor is finally transformed to the global coordinate system by calling a subroutine gblm22.

6. Elastic-Plastic with Isotropic Hardening Implementation

The discussion in this section is focused on the main implementation of elastic, Hill's plasticity and the evolution of the yield surface defined in the new deviatoric plane.

The elastic properties are defined by using the invariant settings of an isotropic function after old stresses have been calculated. These values are then used to calculate the ψ_{ij} tensors with respect to the isoclinic configuration $\bar{\boldsymbol{\Omega}}_i$ and stored locally in a common/scratch1/. Subsequently, the old deviatoric stress tensor and the rate of deformation tensor are transformed to the isoclinic configuration $\bar{\boldsymbol{\Omega}}_i$ in order to define the old deviatoric Mandel stress tensor $\hat{\boldsymbol{\Sigma}}'_0 = \hat{\boldsymbol{\Sigma}}'^n$ and the rate of deformation tensor $\hat{\mathbf{D}}$ in this configuration.

Recalling the discussion in section 4.1, the MTS properties are stored in the main database by using the cm2 array, and further read in the subroutine matin by using five extra material cards. These properties are read in the subroutine sets93 and finally passed to the subroutine f3dm93 by using cm2 array.

The rate of deformation in the isoclinic configuration $\widehat{\mathbf{D}}$ is used to calculate the hardening due to the accumulation of dislocation. Later, the calculation of the saturation threshold stress is further calculated and named dpp. This parameter is first initialised to zero in the subroutine inse93 and passed to the subroutine f3dm93 in the common/aux14/. The value of the MTS flow stress is named sigf and stored locally in the common/scratch1/.

The flow stress of this model is calculated to control the evolution of yield surface in the new deviatoric plane with respect to the isoclinic configuration $\overline{\mathbf{\Omega}}_i$. To be precise, it is adopted as a referential curve to update the current yield stress of the proposed constitutive model using the following equation, named as ak.

$$\hat{\Sigma}_{\mathrm{y}} = \sigma_0 + \frac{\hat{E}_a \hat{E}_T^a}{\hat{E}_a - \hat{E}_T^a} \overline{\widehat{\mathrm{D}}}_p \tag{8}$$

where σ_0, $\hat{E}_a$, $\hat{E}_T^a$ and $\overline{\widehat{\mathrm{D}}}_p$ refer to the yield stress and the elastic modulus in a-direction, the tangent modulus of the MTS flow stress curve and the effective plastic deformation that calculated from the previous timestep respectively. The a-direction denotes a reference direction of this implementation.

The Hill's orthotropy parameters and the MTS parameters are derived using the experimental data in this direction. The value of $\left(\hat{E}_a \hat{E}_T^a / \hat{E}_a - \hat{E}_T^a\right)$ is named as etanmts in the subroutine fdm93. Since the value of $\hat{E}_T^a$ may vary throughout the flow stress curve, this directly reflects the variation of etanmts.

In the following lines of the subroutine f3dm93, the Hill's orthotropic parameters are initialised to construct the invariant-based Hill's matrix $\widehat{\mathbb{h}}$. This matrix is stored in variable dpl. Prior to the next section in this subroutine, the required data are first prepared at this part, where stress and rate of deformation is passed to new variables; from so1…so6 to sigo(1)…sigo(6) and from dd1…dd6 to dt(1)…dt(6). Equally, the increment of the plastic rate of deformation vector is initialised to zero and stored in dp. In the next section, a main loop that performs checking on elastic-plastic parts of the materials under consideration is formulated using the algorithm similar to a radial return algorithm.

In this section, the previous old deviatoric Mandel stress tensor is used to calculate the old equivalent stress (s1old) by using equation (9):

$$\begin{aligned}\overline{\hat{\Sigma}}'^2 = \frac{1}{R+1}\Big(&F'\left(\hat{\Sigma}'_y - \hat{\Sigma}'_z\right)^2 + G'\left(\hat{\Sigma}'_z - \hat{\Sigma}'_x\right)^2 + H'\left(\hat{\Sigma}'_x - \hat{\Sigma}'_y\right)^2 \\ &+ 2L'\hat{\Sigma}'^2_{yz} + 2M'\hat{\Sigma}'^2_{zx} + 2N'\hat{\Sigma}'^2_{xy}\Big)\end{aligned} \tag{9}$$

where F', G' and H' are formulated in terms of Langford parameters R, P, Q_{bc}, Q_{ba}, Q_{ca}:

$$\begin{aligned} F' &= R/\mathrm{P} \\ G' &= 1 \\ H' &= R \end{aligned} \tag{10}$$

Further, using the Langford parameters, L', M' and N' can be defined as

$$L' = \left(Q_{bc} + \frac{1}{2}\right)(R + Z)$$
$$M' = \left(Q_{ba} + \frac{1}{2}\right)(R + Z) \quad (11)$$
$$N' = \left(Q_{ca} + \frac{1}{2}\right)(Z + 1)$$

In the above equation, Z is set equal to $\frac{R}{\mathrm{P}}$. These parameters; $R, \mathrm{P}, Q_{bc}, Q_{ba}, Q_{ca}$ are used in the subroutine fdm93 to characterise the Hill's parameters by using the above equations.

The value of s1old is then compared to the value of ak. The bigger value is selected and named x1, while the increment of the effective plastic deformation is initialised to zero and named as depix. Later, the trial part of the deviatoric Mandel stress tensor (named sigt) is calculated to reflect the definition of the new orthotropic pressure.

The equivalent stress tensor is then calculated by using the trial stress tensor. This equivalent stress is compared with the value of x1 to further identify the state of deformation, either inside (elastic) or outside (plastic) the yield surface.

Strictly speaking, if the equivalent stress sigt is smaller than the value of x1, this means that the increment of the deviatoric Mandel stress tensor is completely inside the yield surface (elastic deformation). No modification is required since the constitutive matrix was correct.

If the trial equivalent stress sigt is larger than the value of x1, then the constitutive matrix needs to be corrected as the stress increment is not completely inside the yield surface (plastic deformation). Two variables were used; fela and fpla. A call to subroutine cepx93 is made to calculate a new elastoplastic constitutive matrix. This subroutine is a copy from subroutine cepx. It was modified to reflect the formulation of the proposed constitutive model using the MTS model to control the evolution of the yield surface in the new deviatoric plane.

The value of $\frac{1}{\mathrm{etanmts}}$ is multiplied by $\frac{1}{R+1}$ and named as ttt. This value is converted into an array of size lnv and then passed to the subroutine cepx93 to calculate the required constitutive matrix. This constitutive matrix is then used to correctly update the deviatoric Mandel stress (stored in sigt) and the related history variables (the equivalent of plastic deformation and its increment, and the increment of plastic deformation).

At the end of the subroutine f3dm93 analysis, a push-forward transformation is performed to bring the Mandel stress back to the current configuration $\boldsymbol{\Omega}_t$. This stress tensor is further combined with the updated orthotropic pressure to finally calculate the update of the full stress tensor.

7. Validation of Numerical Implementation

The validation process is focuses to validate the implementation of the deformation gradient and to ensure an efficient book keeping of the algorithm. Further each part of the formulation and the accuracy of the implemented algorithm is examined, i.e. the validation of orthotropic elastic-plastic behaviour which include strain rate and temperature sensitivity tests. In the next stage, the experimental data of shockwave propagation in orthotropic materials when impacted at high impact velocity is used to validate the above implementation algorithm. A $\mathrm{cm} - \mathrm{g} - \mu\mathrm{s}$ units system is adopted in the involved numerical tests.

7.1. Single Element Analysis of Uniaxial Strain

In the uniaxial strain state, the material is subjected to axial stress and pressure that develop an axial strain, without strain in the radial direction. The confining pressure is increased to force the radial strain back to zero in the case of the radial strain starting to increase, [24]. In addition, the constraints applied in the uniaxial strain test generally can avoid the stress state of the material from reaching the strength limit. Therefore, failure is prevented.

By using a single element analysis for the uniaxial strain test, the validation of the implemented deformation gradient discussed in section 4.2 is greatly simplified. Equally, this analysis also validates the framework of hyperelastic-plastic formulation adopted in the proposed formulation, which related to the deformation gradient. In order to validate the model for the uniaxial strain state, a series of one element analysis are performed. The single element with the node numbering used to define boundary conditions is shown in figure 2. In this model the principle directions of material orthotropy are aligned with the x, y, z axis of the global coordinate system. For brevity, only the test performed in x direction is presented and discussed.

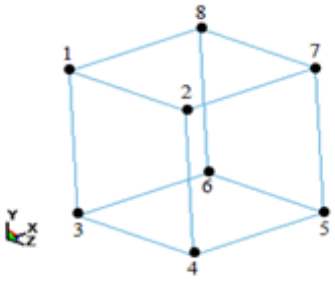

Figure 2. Single Element Configuration

Table 1. Displacements boundary conditions for a Uniaxial Stress and Uniaxial Strain tests in the $\boldsymbol{x}$ direction

Node number	Displacement boundary condition
1	Constrained y and z displacements
2	Constrained y and z displacements
3	Constrained y and z displacements
4	Constrained y and z displacements
5	Constrained x, y and z displacements
6	Constrained x, y and z displacements
7	Constrained x, y and z displacements
8	Constrained x, y and z displacements

The displacement boundary conditions applied in this test are summarised in Table 1. Loading in compression and tension is applied to the elements by prescribing displacement load curves to nodes 1, 2, 3 and 4. The equivalent tests are performed for the y and z directions.

In order to speed up the comparison process, two solid elements with identical geometry, boundary conditions and loading are used in each simulation, as shown in figure 3. In this model one element is assigned the new material model and the other a reference material model available in DYNA3D. This allowed for effective comparison of the new material model against the reference material models. In this work, the uniaxial strain data was analysed by plotting the true stress vs. true strain curves of Material Type 10 and the new material for the x, y, z directions. The value for the material

stiffness in each direction, calculated from the slopes of these curves, is equal to $\boldsymbol{K} + 4\boldsymbol{G}/3$, where $\boldsymbol{K}$ and $\boldsymbol{G}$ are bulk modulus and shear modulus.

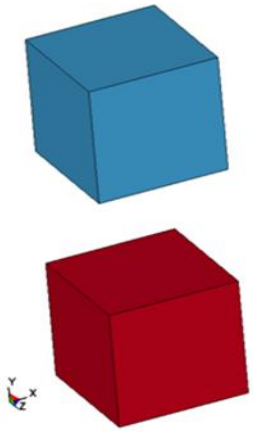

Figure 3. Finite element model for single element analysis

For brevity only single direction used to show the results as shown in figure 4. It is obvious that the stress strain curves for both the new and the reference material are identical in the chosen x direction means that the implementation of the deformation gradient tensor is validated.

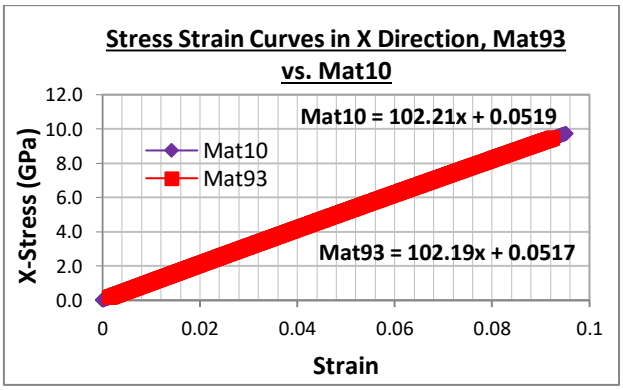

Figure 4. Stress strain curves comparison between Material Type 93 and Material Type 10 in x direction of uniaxial strain

7.2. Single Element Analysis of the Elastic-Plastic Model with Isotropic Plastic Hardening

To validate the implemented algorithm of elastic-plastic and hardening formulation discussed in section 6 to investigate rate sensitivity and temperature sensitivity, the identical set of single element analysis is further conducted. The tensile test data of Aluminium 7010 published in [25] is used at this stage. Assuming the single element represents one of the elements around the gauge length, the uniform plastic deformation is observable using this simplified analysis. The results of this analysis are shown in figures 5, 6, 7 and 8, allow the plastic flow stress response (controlled by MTS model- discussed in section 6) of the constitutive model to be investigated.

Referring these figures, it can be observed that the proposed constitutive model shows a good agreement with the rate and temperature sensitivity of the specimen using the proposed approach. The algorithm of flow stress that formulated as a function of the microstructural state has captured a reasonable relationship between stress, strain rate and temperature of Aluminium 7010.

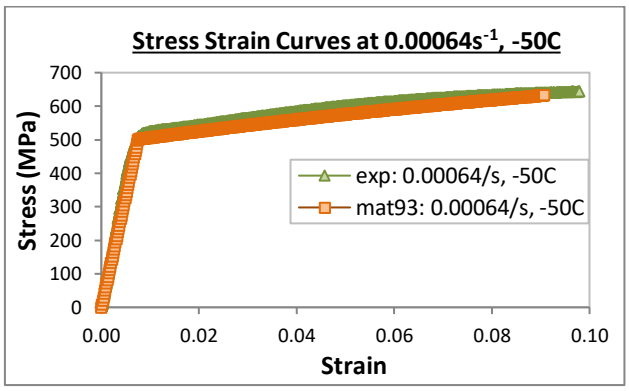

Figure 5. Stress strain curves comparison between Mat93 and experimental data at $\boldsymbol{6.4x10^{-4}s^{-1}}$, $\boldsymbol{-50°C}$

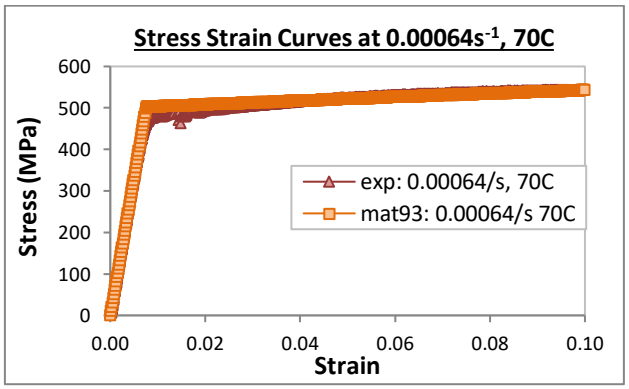

Figure 6. Stress strain curves comparison between Mat93 and experimental data at $\boldsymbol{6.4x10^{-4}s^{-1}}$, $\boldsymbol{70°C}$

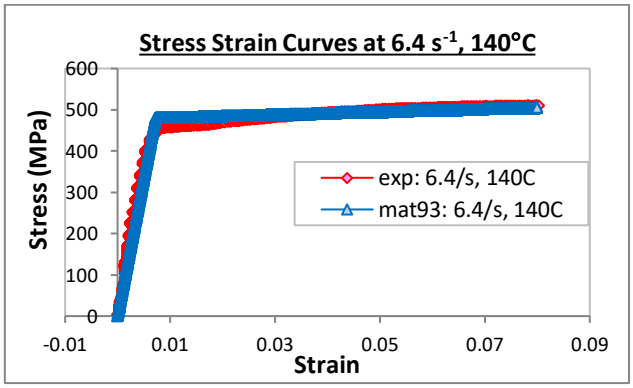

Figure 7. Stress strain curves comparison between Mat93 and experimental data at $\boldsymbol{6.4x10^{-0}s^{-1}}$, $\boldsymbol{140°C}$

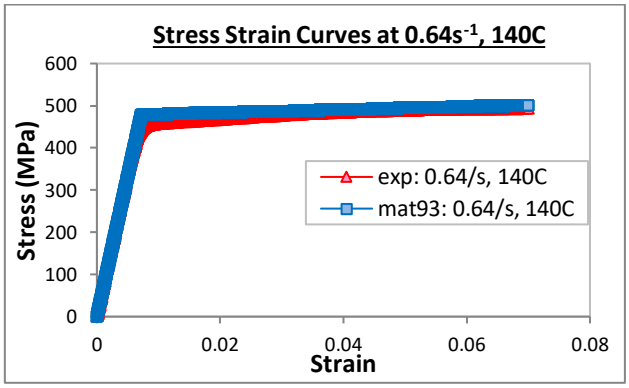

Figure 8. Stress strain curves comparison between Mat93 and experimental data at $\boldsymbol{6.4x10^{-1}s^{-1}}$, $\boldsymbol{140℃}$

Generally, it can be concluded that increasing strain rate increases the flow stress, while increasing temperature decreases the flow stress. In other words, the saturation stress of the newly implemented algorithm of the proposed material model increases with increasing strain rate and decreases with increasing temperature. Up to this stage, the algorithm of the proposed constitutive formulation for orthotropic materials is almost completely established.

7.3. Plate Impact Test

Plate Impact then is used to ensure an efficient book-keeping of the algorithm to deal with multiple elements analysis and to check its capability to capture shockwave propagation in orthotropic materials. Figure 9 shows the configuration of the Plate Impact test simulation. It can be observed that the test consists of three parts of rectangular bars with $4x4$ solid elements for its cross section (XY plane). The first bar represents the PMMA block, while the second and third bars refer to the test specimen and flyer respectively. The mesh of this simulation is set to allow a 1D wave to propagate along the length of the bars when the impact happens. From this figure, it is noticed that symmetrical planes are adopted on all sides of the bars.

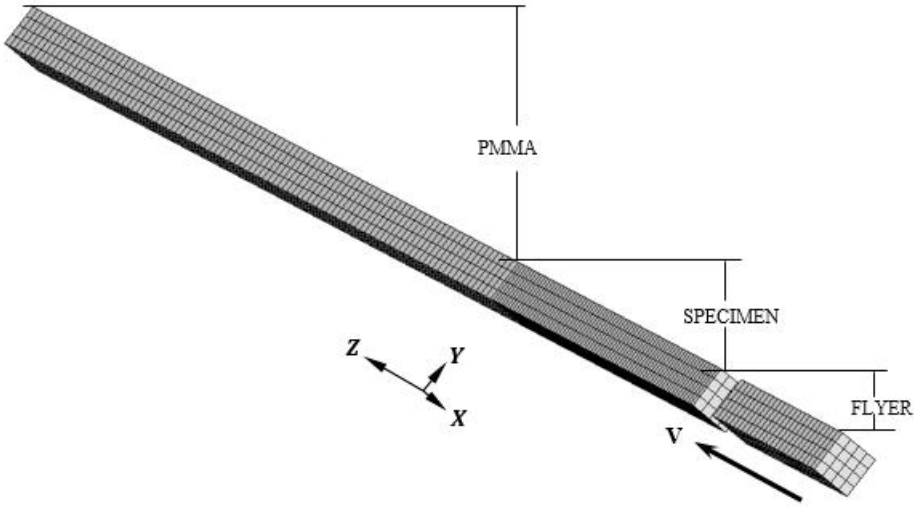

Figure 9. Configuration of the Plate Impact test simulation

To ensure that no release wave is reflected from the back of the PMMA block into the test specimen, a non-reflecting boundary condition is applied to the back of this block (PMMA). In addition, the flyer, test specimen and PMMA bars are modelled with 25 solid elements (2.5mm in length), 75 solid elements (10mm in length) and 100 solid elements (12mm in length) respectively,

parallel to the impact axis (Z axis). A contact interface is defined in between the flyer and the test specimen. To record the stress time histories of the impact, a time history block is defined in the elements at the top of PMMA bar.

In this analysis, the longitudinal stress (Z stress) in the elements at the top of the PMMA bar is compared with the experimental data with respect to the short transverse and the longitudinal (rolling) directions of the specimen. The flyer is defined as Aluminium $6082-T6$. Both the flyer and the PMMA blocks are assigned with DYNA3D's Material Type 10 (Isotropic-Elastic-Plastic-Hydrodynamic). The Gruneisen equation of state is adopted to appropriately represent the shock loading developed in this test. In addition, three different impact velocities are performed in these analyses 234ms^{-1}, 450ms^{-1} and 895ms^{-1}. By setting the material axes definition as AOPT 2 (globally orthotropic), the following results are obtained. It can be observed in figure 10, figure 11, figure 12, figure 13, figure 14 and figure 15 that the elastic-plastic loading-unloading behaviours of the $\text{Al}7010$ are well captured by the implemented algorithm of the proposed constitutive model. A slope that is developed in the initial increment of the longitudinal stress represents the Hugoniot Elastic Limit (HEL). Without knowing the error that might happen in the experimental test, such as an inaccuracy of the gauge used to measure the longitudinal stress etc., a slight difference between the new constitutive model's HEL and the values obtained experimentally is absolutely acceptable. In addition, a different HEL value obtained in each direction is a sign of an adequate anisotropy level of the material under consideration.

The width of the generated pulses in each analysis is reasonably agreed with the experimental test data. Furthermore, very close Hugoniot stress levels between the new constitutive model and the experimental data proved the capability of the newly implemented orthotropic pressure discussed in section 5.2 to capture shockwaves in orthotropic materials.

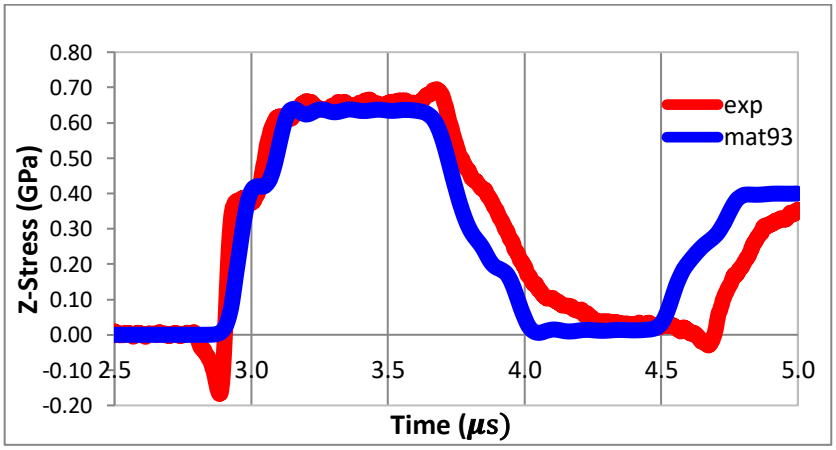

Figure 10. Longitudinal stress (Z stress) comparison at $\mathbf{234ms^{-1}}$ in longitudinal direction

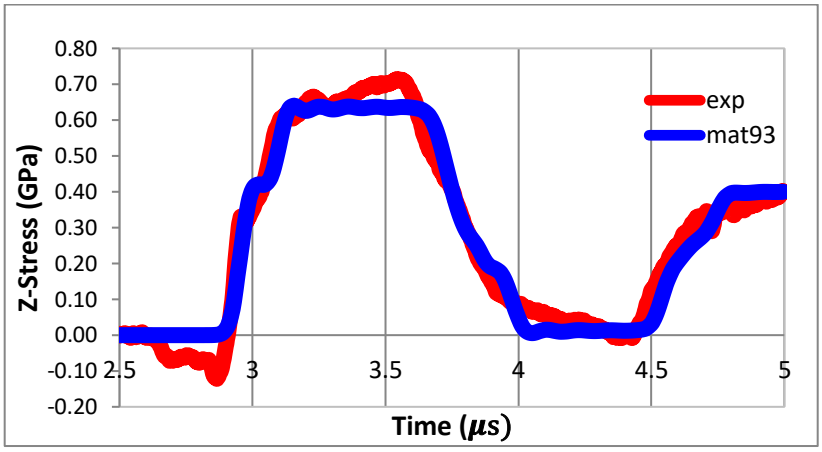

Figure 11. Longitudinal stress (Z stress) comparison at $\mathbf{234ms^{-1}}$ in transverse direction

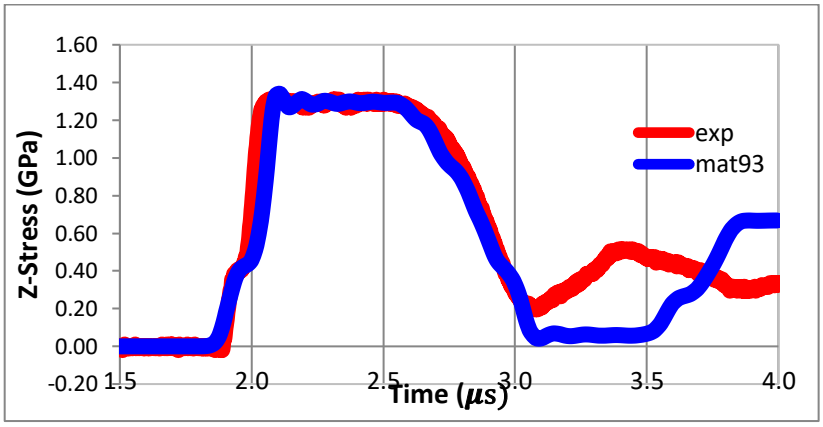

Figure 12. Longitudinal stress (Z stress) comparison at $\mathbf{450ms^{-1}}$ in longitudinal direction

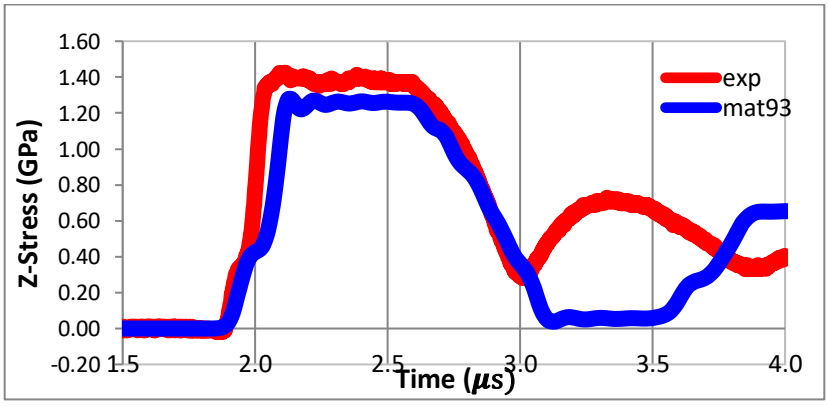

Figure 13. Longitudinal stress (Z Stress) comparison at $\mathbf{450ms^{-1}}$ in transverse direction

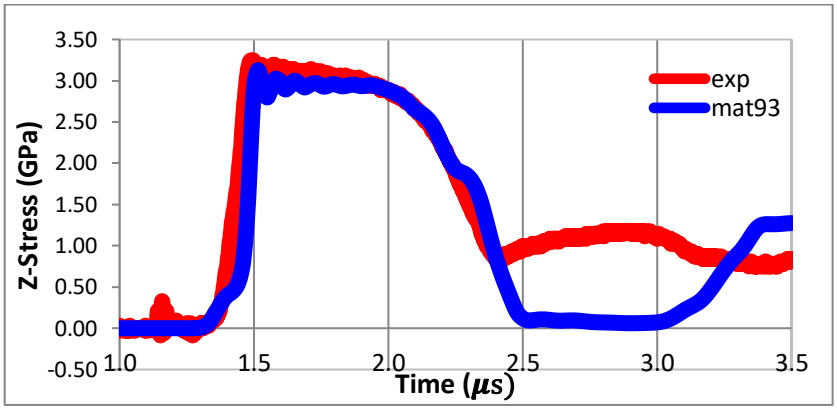

Figure 14. Longitudinal stress (Z stress) comparison at $\mathbf{895ms^{-1}}$ in longitudinal direction

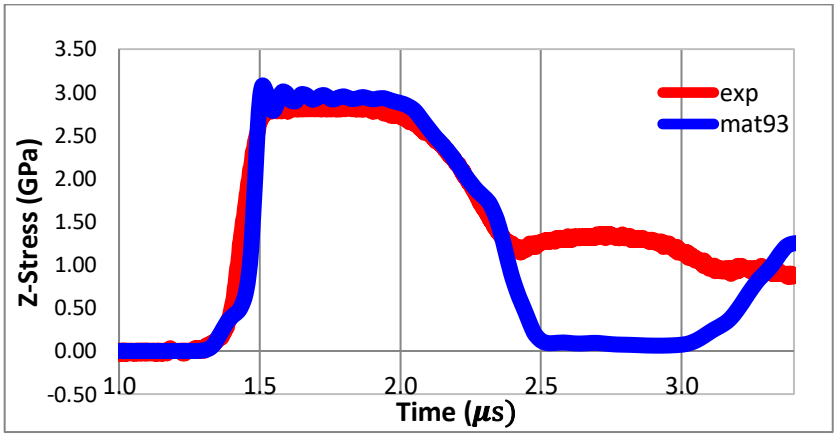

Figure 15. Longitudinal stress (Z stress) comparison at $\mathbf{895ms^{-1}}$ in transverse direction

In this analysis, it can be clearly seen that the tensile wave failure or spall (demonstrated by the reloading of the longitudinal stress after the first loading-unloading pulse) is not generated in the specimen when impacted with a lower impact velocity ($234ms^{-1}$). However, a clear spall criterion can be observed when higher impact velocities ($450ms^{-1}$ and $895ms^{-1}$) are applied. Such behaviour could not be captured by the newly implemented Material Type 93 in the LLNL -DYNA3D code due to no damage and failure models in the proposed formulation of this constitutive model.

8. Conclusion

The framework of new constitutive model implementation into the LLNL-DYNA3D code is concisely discussed in this paper. The structure of the code and its data handling is first identified correctly to define subroutines involve in the implementation process. In this paper, the existing Material Types 33 and Material Type 97 in the LLNL-DYNA3D have been taken as references to start the implementation. This paper also emphasizes the importance to perform a preliminary review on the selected code for implementation such as types of available constitutive models, EOSs, etc. The approach discussed in this paper is certainly useful to guide other researchers to implement finite strain based constitutive models into the LLNL-DYNA3 code. The proposed framework also can be a guideline to identify the required implementation works in the other finite element codes. The results show that the chosen approach for algorithm implementation is appropriate.

9. References

[1] Vignjevic, Bourne, N. K., Millett, J. C. F. and De Vuyst, T. 2002 Effects of orientation on the strength of the aluminum alloy 7010-T6 during shock loading: Experiment and simulation, *Journal of Applied Physics*, vol. 92, no. 8, pp. 4342-4348

[2] Sinha, S. and Ghosh, S. 2006 Modeling cyclic ratcheting based fatigue life of HSLA steels using crystal plasticity FEM simulations and experiments, *International Journal of Fatigue*, vol. 28, no. 12, pp. 1690-1704

[3] Meredith, C. S. and Khan, A. S. 2012 Texture evolution and anisotropy in the thermo-mechanical response of UFG Ti processed via equal channel angular pressing, *International Journal of Plasticity*, vol. 30-31, pp. 202-217

[4] Khan, A. S. and Meredith, C. S. 2010 Thermo-mechanical response of Al 6061 with and without equal channel angular pressing (ECAP), *International Journal of Plasticity*, vol. 26, no. 2, pp. 189-203

[5] Furnish, M. D. and Chhabildas, L. C. 1998 Alumina strength degradation in the elastic regime, *AIP Conference Proceedings,* vol. 429, no. 1, pp. 501-504

[6] Minich, R., Cazamias, J., Kumar, M. and Schwartz, A. 2004 Effect of microstructural length scales on spall behaviour of copper, *Metallurgical and Materials Transactions A*, vol. 35, no. 9, pp. 2663-2673

[7] Kanel, G. I., Zaretsky, E. B., Rajendran, A. M., Razorenov, S. V., Savinykh, A. S. and Paris, V. 2009 Search for conditions of compressive fracture of hard brittle ceramics at impact loading, *International Journal of Plasticity*, vol. 25, no. 4, pp. 649-670

[8] Zaretsky, E. B. and Kanel, G. I. 2011 Plastic flow in shock-loaded silver at strain rates from 10[sup 4]s[sup - 1] to 10[sup 7]s[sup - 1] and temperatures from 296 K to 1233 K, *Journal of Applied Physics*, vol. 110, no. 7, pp. 073502

[9] Khan, A. S., Kazmi, R., Pandey, A. and Stoughton, T. 2009 Evolution of subsequent yield surfaces and elastic constants with finite plastic deformation. Part-I: A very low work hardening aluminum alloy (Al6061-T6511), *International Journal of Plasticity*, vol. 25, no. 9, pp. 1611-1625

[10] Nakamachi, E., Tam, N. N. and Morimoto, H. 2007 Multi-scale finite element analyses of sheet metals by using SEM-EBSD measured crystallographic RVE models, *International Journal of Plasticity*, vol. 23, no. 3, pp. 450-489

[11] Khan, A. S., Kazmi, R. and Farrokh, B. 2007 Multiaxial and non-proportional loading responses, anisotropy and modeling of Ti–6Al–4V titanium alloy over wide ranges of strain rates and temperatures, *International Journal of Plasticity,* vol. 23, no. 6, pp. 931-950

[12] Khan, , A. S., Kazmi, R., Farrokh, B. and Zupan, M. 2007 Effect of oxygen content and microstructure on the thermo-mechanical response of three Ti–6Al–4V alloys: Experiments and modeling over a wide range of strain-rates and temperatures, *International Journal of Plasticity,* vol. 23, no. 7, pp. 1105-1125

[13] Sitko, M., Skoczeń, B. and Wróblewski, A. 2010 FCC-BCC phase transformation in rectangular beams subjected to plastic straining at cryogenic temperatures, *International Journal of Mechanical Sciences,* vol. 52, no. 7, pp. 993-1007

[14] Vignjevic R., Djordjevic N. and Panov V. 2012 Modelling of Dynamic Behaviour of Orthotropic Metals Including Damage and Failure, *International Journal of Plasticity*, vol. 38, pp.47–85

[15] Cazacu, O., Barlat, F. 2003 Application of representation theory to describe yielding of anisotropic aluminum alloys, *International Journal of Engineering Science,* 41, 1367–1385

[16] Mohd Nor M. K., Vignjevic R., Campbell J. 2013 Modelling of Shockwave Propagation in Orthotropic Materials, *Applied Mechanics and Materials*, Vol. 315, pp 557-561

[17] Mohd Nor M. K. 2016 Modeling of Constitutive Model to Predict the Deformation Behaviour of Commercial Aluminum Alloy AA7010 Subjected to High Velocity Impacts, *ARPN Journal of Engineering and Applied Sciences*, Vol. 11(4), pp 2349-2353

[18] M.K. Mohd Nor, Modeling Inelastic Behaviour of Orthotropic Metals In a Unique Alignment of Deviatoric Plane Within the Stress Space, International Journal of Non-Linear Mechanics, http://dx.doi.org/10.1016/j.ijnonlinmec.2016.09.011
[19] Campbell, J. 1998 Lagrangian hydrocode modeling of hypervelocity impact on spacecraft, PhD Dissertation, Cranfield University, Cranfield
[20] De Vuyst, T. 2003 Hydrocode modelling of water impact, PhD Dissertation, Cranfield University, Cranfield
[21] Lin, J. I. 2004 DYNA3D: A Nonlinear, Explicit, Three-Dimensional Finite Element Code for Solid and Structural Mechanics User Manual, Lawrence Livermore National Laboratory
[22] Hallquist, J. 1983 Theoretical manual for DYNA3D, Technical report, Lawrence Livermore National Laboratory
[23] Vignjevic, R., Campbell, J., Bourne, N. K., Djordjevic, N., 2007 Modelling Shock Waves in Orthotropic Elastic Materials – *Conference on Shock Compression of Condensed Matter*, Hawaii, June,
[24] Thomas, M. A., Chitty, D. E., Gildea, M. L. and T'Kindt, C. M. 2008 Constitutive Soil Properties for Cuddeback, Applied Research Associates, Inc., Albuquerque, New Mexico
[25] Panov, V. 2006 Modelling of behaviour of metals at high strain rates, PhD dissertation, Cranfield University, Cranfield

Acknowledgments
The authors wish to convey a sincere gratitude to Universiti Tun Hussein Onn Malaysia (UTHM) and Ministry of Higher Education Malaysia (MOHE) for providing the financial means during the preparation to complete this work under Fundamental Research Grant Scheme (FRGS), Vot 1547.